

**Mo-99 2016 TOPICAL MEETING ON
MOLYBDENUM-99 TECHNOLOGICAL DEVELOPMENT**

**SEPTEMBER 11-14, 2016
THE RITZ-CARLTON
ST. LOUIS, MISSOURI**

**Chemical Processing for Non-uranium Production of
 $^{99}\text{Mo}/^{99\text{m}}\text{Tc}$**

P. Tkac, K.E. Wardle, M.A Brown, A. Momen, D.A. Rotsch, J.M Copple, S.D. Chemerisov, R. Gromov, and G.F. Vandegrift
Nuclear Engineering Division
Argonne National Laboratory, 9700 S. Cass Ave., 60439 Argonne – United States

ABSTRACT

A non-uranium pathway for production of hundreds of curies of $^{99}\text{Mo}/^{99\text{m}}\text{Tc}$ requires enriched ^{98}Mo or ^{100}Mo . An estimated cost for >95% enriched $^{98/100}\text{Mo}$ is about \$1,000/g. To meet supply demands, kilogram quantities are required. Due to the high cost for the enriched target material, potential manufacturers require a means to efficiently recycle the enriched Mo into new targets as part of the complete production scheme. Impurities present in the enriched material, as well as those introduced during post-irradiation processing or recycling, need to be closely monitored. Experimental results on irradiation of Mo targets, dissolution studies to optimize the target properties, and a solvent extraction approach to recycle enriched Mo material will be presented.

1. Introduction

Molybdenum-99 is an important medical isotope. Currently, the majority of ^{99}Mo is produced by fissioning of ^{235}U in high enriched uranium (HEU) in nuclear reactors, because of its very high fission yield (6.1%) and high thermal neutron fission cross section. However, the majority of reactors currently used for production of medical isotopes have been in operation for several decades. Other technologies have been recently proposed for production of this isotope. They include production of ^{99}Mo by $^{100}\text{Mo}(\gamma,n)^{99}\text{Mo}$ reaction [1, 2] using an electron accelerator, and cyclotron production of $^{99\text{m}}\text{Tc}$ using $^{100}\text{Mo}(p,2n)^{99\text{m}}\text{Tc}$ [3-5]. There has been much interest in direct production of $^{99\text{m}}\text{Tc}$ using medical cyclotrons due to their availability in many countries. Current feasibility studies have demonstrated the production of ~5.7 Ci/h of $^{99\text{m}}\text{Tc}$ with ^{100}Mo enriched targets using medium-energy cyclotrons at 200 μA and 30-12 MeV (1.8 kW) [4]. Another alternative is production of ^{99}Mo in a reactor using enriched ^{98}Mo targets by $^{98}\text{Mo}(n, \gamma)^{99}\text{Mo}$ reaction. The typical yield with natural Mo in the thermal flux of a research reactor ($5 \times 10^{13} \text{n/cm}^2\text{-s}$) is ~0.8 Ci/h of ^{99}Mo per 500 g of target, while high flux reactors with >95% enriched ^{98}Mo can produce ~32 Ci/h of ^{99}Mo for the same size of Mo target [4, 6].

NorthStar Medical Technologies, LLC (NorthStar) is pursuing near- and long-term pathways for production of ^{99}Mo . The former pathway produces ^{99}Mo by the $^{98}\text{Mo}(\text{n},\gamma)^{99}\text{Mo}$ reaction at the University of Missouri Research Reactor (MURR). The latter pathway produces ^{99}Mo via the photonuclear reaction $^{100}\text{Mo}(\gamma,\text{n})^{99}\text{Mo}$ from the irradiation of enriched molybdenum targets by an electron accelerator. Processing of irradiated targets, from either production mode, requires dissolution in hydrogen peroxide and conversion of the dissolved material into a highly alkaline solution for separation of Tc and Mo with the RadioGenix® generator. Currently, NorthStar is using pressed and sintered Mo disk as targets. It has been demonstrated [7-10] that the particle size of Mo metal used for production of targets, sintering conditions, open porosity, and thickness of the sintered Mo targets can play important roles in the dissolution characteristics. Argonne National Laboratory (Argonne) in collaboration with Oak Ridge National Laboratory (ORNL) has investigated how these important disk properties affect the dissolution properties of Mo disks.

All alternative routes for production of ^{99}Mo , as well as the cyclotron-driven direct production of $^{99\text{m}}\text{Tc}$ mentioned above, require use of enriched ^{98}Mo or ^{100}Mo for efficient production. Enriched molybdenum (>95% enriched ^{100}Mo) currently costs \$850-3000 per gram [11]. Due to this very high cost, potential manufacturers require ways to efficiently recycle it. Besides high recovery yields, equally important is finding a particle size for the recycled Mo powder that is suitable for production of recycled Mo targets that have high enough theoretical density and good dissolution characteristics for quick post-irradiation processing.

Here, we present the latest experimental results on dissolution of small-scale sintered and laser melt 3D-printed Mo disks, irradiations of sintered Mo disks, and recycle of Mo material by using solvent extraction.

2. Experimental

2.1 Linac irradiations

Four irradiations of ultra-high purity (UHP) natural Mo targets and one irradiation using 97.4% ^{100}Mo enriched material (Trace Science) were performed in FY 2016. The irradiation conditions and masses of the Mo targets are listed in Table 1.

Table 1. Irradiation conditions for sintered Mo targets

Material	Mass (g)	Energy (MeV)	Current (μA)	Average power (kW)	Irradiation time (h)
UHP natural Mo	1.13	40	135	5.4	8
UHP natural Mo	1.05	40	135	5.4	10.8
UHP natural Mo	1.06	40	135	5.4	10.4
UHP natural Mo	1.03	40	135	5.4	10.4
97.4% ^{100}Mo	2.09	40	100	4.0	5.5

The irradiated Mo disks were dissolved in either 50% hydrogen peroxide stabilized with Sn (Aqua Solutions, Inc., #H3050-4L) or 30% non-stabilized peroxide (Acros Organics, #411885000) to investigate if the presence of Sn as a stabilizer affects the radiochemical purity of the product by interaction of Sn with Mo or Tc. After a complete dissolution, KOH (Alfa Aesar, #44273) was added to convert the Mo into K_2MoO_4 in 5M KOH solution. Excess of peroxide was eliminated by evaporation, and the volume was adjusted by addition of water to

make 0.2 g-Mo/mL. Due to the presence of impurities in the ^{100}Mo -enriched material (540 ppm Fe, 75 ppm W, 65 ppm Cr, 39 ppm Ni, 15 ppm Cu, and 11 ppm Ge), an orange precipitate was observed after addition of the KOH; therefore, after cooling, the solution was filtered through a 0.3- μm filter. Thin layer chromatography (TLC) was performed with ITLC-SG strips (Agilent Technologies, SGI0001) and 0.1M sodium carbonate as a mobile phase. A few microliters of the Mo solution was added to the paper and was allowed to dry. Chromatograms were developed in 0.1M sodium carbonate solution. Since the solution is colorless, the front of the TLC was marked with droplet of phenolphthalein to visually observe when the mobile phase reached the front of the chromatogram. This was indicated by a purple color on the front of the chromatogram (Figure 1). Next, the strips were allowed to dry, cut into 11 fractions, and gamma counted. Gamma counting was performed with an HPGe detector.



Figure 1. Spotting of mobile phase (Na_2CO_3) on TLC using phenolphthalein

2.2 Dissolution of sintered and laser melt 3D-printed Mo disks

Sintered Mo disks and 3D-printed disks (laser-melt produced) were fabricated by ORNL. Small disks (<2 g) were dissolved in 40 mL of 50% hydrogen peroxide (Aqua Solutions, Inc., #H3050-4L) preheated to 70°C (unless stated otherwise) in a 250 mL beaker. Larger disks were dissolved in a 2 L reaction vessel. The sintered and 3D-printed disks are shown in Figure 2.

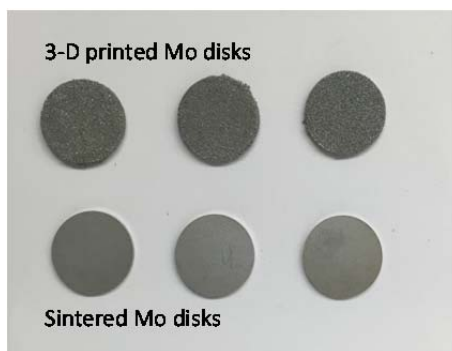


Figure 2. Photograph of 12x1mm sintered and 12.4x1.5-1.9mm 3-D printed Mo disks

Results on a large-scale dissolution experiments with 600 g of sintered Mo disks are presented in a separate paper of this proceedings [12].

2.3 Recycle of Mo using solvent extraction

A scheme for the recycle process, which recovers Mo from the spent generator solution to Mo metal powder, is illustrated in Figure 3. In this scheme, the alkaline solution is acidified with hydrochloric acid (HCl), which acts to precipitate a large fraction of potassium as KCl. The resulting solution is then contacted by the tributyl phosphate (TBP) solvent, which extracts molybdenum as a molybdenyl chloride salt but does not extract KCl. Molybdenum is then stripped from the solvent by using ammonium hydroxide. This solution is then evaporated, which precipitates molybdenum as ammonium heptamolybdate (AHM: $(\text{NH}_4)_6\text{Mo}_7\text{O}_{24} \cdot x\text{H}_2\text{O}$) and ammonia as ammonium chloride (NH_4Cl). The solid is washed with ethanol (EtOH), which dissolves the NH_4Cl away from the AHM. The AHM can be reduced directly to Mo metal by heating in a hydrogen-containing stream.

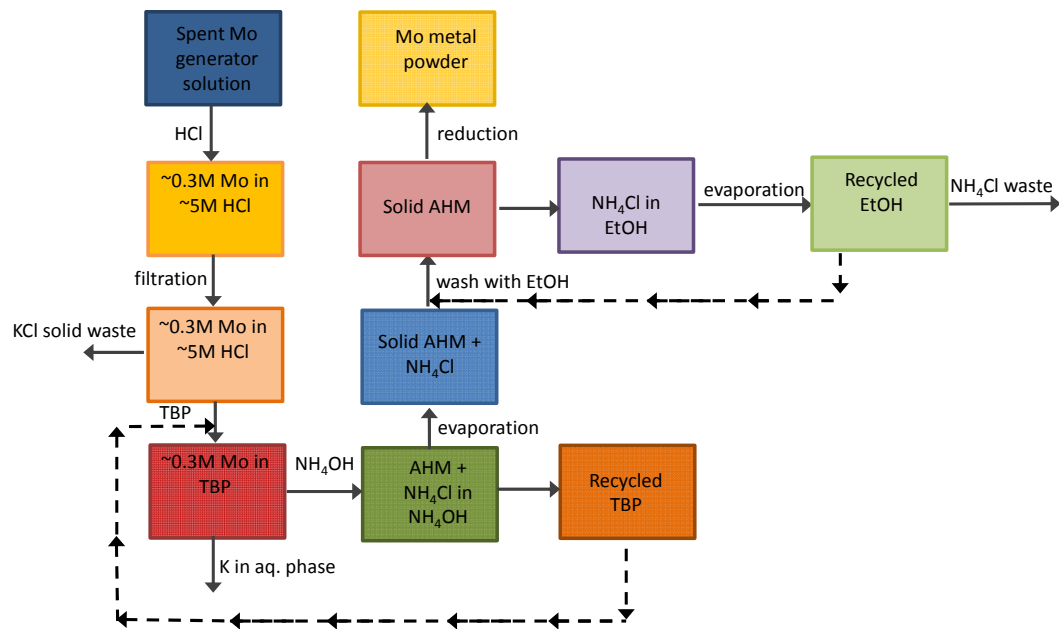


Figure 3. Scheme of Mo recycle process

Large-scale solvent extraction experiments were performed by pouring 50% TBP in 1-octanol in 12 L high-density polyethylene (HDPE) bottles, and separating the phases by using a 5 L separatory funnel. In these experiments, 700 mL of spent generator solution surrogate (0.2 g-Mo/mL in 5M KOH) was acidified with concentrated HCl. During the acidification process, a white solid containing KCl was precipitated and filtered after cooling to room temperature by using a coarse frit under vacuum. Solid KCl was washed with ~100 mL of concentrated HCl to remove any Mo. The resulting yellow solution containing Mo was further diluted with water to make ~0.33M Mo in ~5M HCl. After extraction of Mo by TBP, the organic phase was scrubbed with 4-5M HCl, and then Mo was stripped with NH_4OH . Stripped solution was then evaporated using a rotary evaporator and a solid mixture of AHM, and ammonium chloride (NH_4Cl) was obtained. Due to its corrosive properties, ammonium chloride needs to be removed before reduction of AHM into Mo metal. The mixture of NH_4Cl and AHM was mixed with 80% ethanol to remove NH_4Cl , while AHM stayed on the filter as solid. A test for the presence of chloride in the AHM was performed by taking a small aliquot of AHM, dissolving it in water, and acidifying with HNO_3 . In the test, a few drops of AgNO_3 solution were added. If a white precipitate or

cloudy solution formed after addition of AgNO_3 , more washing steps with ethanol were performed. After the final wash, the AHM was air dried. Samples of AHM were sent to ORNL for reduction.

3. Results and Discussion

3.1 Radiochemical purity of Mo/Tc solution

In FY 2015, we performed several irradiations using enriched ^{100}Mo and natural Mo. Corrosion was observed on the irradiated Mo disks and target housing, possibly due to corrosion of the carbon-steel shielding enclosure or the He cooling loop. The solution obtained after the dissolution of irradiated targets in peroxide, conversion into ~5M KOH, and filtration through a 0.3- μm filter was a light orange color—indicating the presence of impurities (most likely iron). Radiochemical purity (RCP) TLC tests performed with the undiluted Mo solution [7] did not meet the specifications, and lower and inconsistent $^{99\text{m}}\text{Tc}$ yields were observed when the solution was loaded into a TechneGen generator (an older model of RadioGenixTM). Therefore, in FY 2016, several irradiations were undertaken with UHP natural Mo and ^{100}Mo enriched disks without using the He cooling system. The Mo target was wrapped in an Al foil and placed behind the converter. These tests were performed to learn if the presence of Sn introduced during the dissolution process by using Sn-stabilized peroxide affected the radiochemical purity of Mo and Tc in the final product.

Gamma counting results from solutions obtained after dissolution of irradiated Mo targets in peroxide and conversion into 0.2 g-Mo/mL in 5M KOH solution are presented in Table 2.

Table 2. Gamma-counting and RCP-test results

Sample	Mo (g)	Activity at EOB (mCi)						$R_F=0.9\pm0.1$		H_2O_2 used
		^{99}Mo	^{90}Mo	$^{93\text{m}}\text{Mo}$	$^{95\text{m}}\text{Nb}$	^{95}Nb	^{96}Nb	^{99}Mo	$^{99\text{m}}\text{Tc}$	
1	UHP, 1.13	16.5	2.8	ND	0.79	0.11	2.34	91.3%*	89.5%*	30% NS
2	UHP, 1.05	15.3	1.8	0.01	0.79	0.07	1.98	99.7%	96.5%	50% Sn-stab
3	UHP, 1.06	13.5	2.2	ND	0.72	0.06	1.89	99.5%	95.8%	50% Sn-stab
4	UHP, 1.03	16.1	2.5	ND	0.83	0.07	2.22	99.3%	94.6%	30% NS
5	^{100}Mo , 2.09	123.2	ND	0.04	0.05	ND	ND	98.4%	98.3%	50% Sn-stab

EOB – end of bombardment; ND – below detection limit; * undiluted solution of Mo in 5M KOH; NS – non stabilized; Sn-stab – tin stabilized.

A typical chromatogram obtained after spotting 20 μL of 3.5 \times diluted solution of Mo in 5M KOH with water is shown in Figure 4.

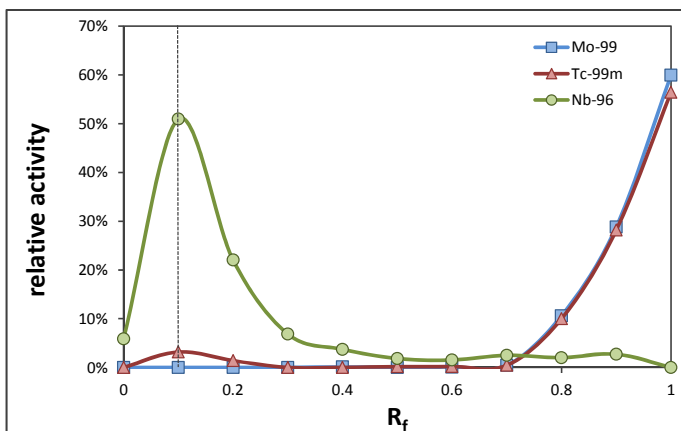


Figure 4. Retention factors for Mo, Tc, and Nb after spotting 20 μL of 3.5 \times diluted solution of Mo in 5M KOH with water on TLC (sample 4, Table 2)

After dissolution of all UHP disks, the solution obtained after addition of KOH was clear and colorless. However, dissolution of ^{100}Mo enriched material and conversion to molybdate solution in 5M KOH led to formation of an orange precipitate, which was removed by filtration. After the filtration, a clear and colorless solution was obtained and sent to NorthStar for further analyses. Results from RCP tests performed on all solutions (Table 2) indicate that no radiochemical impurities are present in the final solutions. Note that for samples 3 and 4 (Table 2) some portion of Tc was found at $R_f=0.1$, which corresponds to a maximum for Nb retention factor (see Figure 4). It is unclear, however, if any interaction between Tc and Nb (or other impurities) occurs. Based on these experiments, we concluded that introduction of Sn by using Sn-stabilized peroxide, or the presence of up to 500 ppm Fe and other impurities (see experimental section) in the enriched ^{100}Mo target, does not affect the radiochemical purity of the product. Therefore, it is likely that, during the FY 2015 production runs, impurities that affected the RCP were introduced during the irradiation (corrosion found on the target). Therefore, for all future irradiations using the He cooling system, precautions should be made to eliminate the source of impurities during the irradiation.

3.2 Dissolution of sintered and laser melt 3D-printed Mo disks

We previously demonstrated [7-10] that the particle size of Mo metal used for production of targets, sintering conditions, open porosity, and thickness of the sintered Mo targets can play important roles in the dissolution characteristics. Argonne in collaboration with ORNL has investigated the dissolution properties of sintered and 3D-printed Mo disks. Because 3D printing allows for more flexibility in target design, where an entire target, including the housing, can be fabricated from Mo, ORNL decided to explore options for 3D-printed targets for accelerator production of ^{99}Mo . Also, much thinner target components can be achieved by 3D printing compared to the traditional press-and-sinter approach. It is, therefore, important to investigate the dissolution properties of 3D-printed targets and compare them to sintered targets. The 3D printing of Mo is currently performed at ORNL, and although this process is in the early stage of development, it is a promising technique for future target design.

When H_2O_2 was preheated to 70°C, the sintered Mo disks dissolved quickly (as expected based on previous experiments). When room temperature (24°C) peroxide was used, an activation period was required to produce enough heat to increase the peroxide temperature until the disks

started to dissolve vigorously. The characteristics of sintered Mo disks and dissolution times are listed in Table 3. Dissolution rates are in the range of ~0.76-1.05 g/min.

Table 3. Disks characteristics and dissolution results for sintered Mo disks in 40 mL of 50% H₂O₂

Disk	Mass (g)	Theor. Density (%)	Open Porosity (%)	Diameter (mm)	Thickness (mm)	50% H ₂ O ₂ , temperature (°C)	Diss. time (min)	Diss. rate (g/min)
S50-12A-5	0.986	87.9%	7.9	11.99	0.94	70°C	1.25	0.79
S50-12A-7	1.008	89.1%	2.7*	12.01	0.94	70°C	1.33	0.76
S50-12A-8	0.994	87.9%	7.8	12.01	0.97	24°C	6.25	0.16*
S50-12A-10	0.994	86.7%	8.3	12.01	0.97	70°C	1.00	0.99
S50-12B-2	1.052	87.4%	8.6	11.99	1.05	70°C	1.00	1.05
S50-12B-4	1.048	87.3%	8.3	11.99	1.06	24°C	4.00	0.26 ⁺
S50-12B-21	1.055	87.1%	8.0	11.99	1.05	70°C	1.33	0.79

*Once starting to dissolve after an activation period (5 min), the dissolution rate is 0.789 g/min.

⁺Once starting to dissolve after an activation period (3 min), the dissolution rate is 1.05 g/min.

In general, laser melt 3D-printed disks dissolved slower compared to sintered Mo disks. After 1-2 min of dissolution, the disks broke down into very small pieces, and the dissolution of small particles took a longer time to completely dissolve (several additional minutes) where additional heating was provided by a hot plate. Some of the fine particles looked like tiny wires (disk Mo-45-16-9, see Figure 5).



Figure 5. Photograph of residual small particles that form during the dissolution of laser melt 3D-printed Mo disks

The characteristics of laser melt 3D-printed Mo disks and their dissolution times are listed in Table 4. Dissolution rates are in the range of ~0.1-0.25 g/min.

Table 4. Disk characteristics and dissolution results for laser melt 3D-printed Mo disks in 40 mL of 50% H₂O₂

Disk	Mass (g)	Theor. Density (%)	Open Porosity (%)	Diameter (mm)	Thickness (mm)	50% H ₂ O ₂ , temperature (°C)	Diss. time (min)	Diss. rate (g/min)
Mo45-16-3	1.647	90.0%	9.8	12.40	1.90	70°C	10.00	0.165
Mo45-16-9	1.738	89.0%	10.4	12.40	1.90	70°C	18.00	0.097
Mo45-16-10	1.715	89.9%	9.5	12.40	1.90	70°C		
Mo45-23-1	1.266	89.5%	8.5	12.40	1.50	24°C	6.00	0.211*
Mo45-23-2	1.284	91.0%	7.5	12.40	1.50	70°C	+	+
Mo45-23-7	1.272	90.3%	6.7	12.40	1.50	70°C	5.00	0.254

*Dissolution started in 24°C peroxide; however, fine particles had to be dissolved with additional heat using hot plate.

[†] It was difficult to determine exact time of dissolution because of numerous bubbles.

An interesting observation (based on very limited number of disks) was that for the laser melt disks, the dissolution rate dependency on open porosity was the reverse of that for sintered disks. The disk with the highest open porosity (10.4%) dissolved with the lowest dissolution rate (below 0.1 g/min), while the disk with lowest open porosity (6.7%) dissolved the fastest (0.254 g/min). A possible explanation is that the laser melt disks with large open porosity contain fused particles with different macro- and microstructure that required a longer time to dissolve.

3.3 Recycle of Mo using solvent extraction

Much attention has recently been devoted to recycle pathways to recover valuable enriched Mo material. Bénard et al. [13] and Gagnon et al. [14] reported 85 and ~87% recovery yields, respectively. Recently, we reported ~95% total recovery yields for recycle of enriched Mo by using a highly alkaline spent generator system (RadioGenix® from NorthStar) and a precipitation technique [15]. The process was performed with up to 260 g of Mo and can be scaled up for processing of up to 400 g of Mo. Besides high recovery yields, an equally important aspect of developing a recycle method is achieving a particle size of the recycled Mo powder that is suitable for production of Mo targets that have high enough theoretical density and good dissolution characteristics for quick post-irradiation processing. If very fine Mo powder is used for production of sintered Mo targets, high theoretical density disks can be manufactured by the classic sinter-press technique. However, depending on the sintering temperatures used for the production of Mo disks, the dissolution rates can be severely affected and lead to prolonged dissolution times [9, 10]. On the other hand, a very coarse Mo powder material can lead to lower theoretical densities of the pressed targets, and the necessity to mill the material into desired particle size will lead to losses of enriched material or the requirement for further processing of the Mo material in an undesired particle size range.

Although the precipitation technique for Mo recycle [15] leads to high recovery yields, we found that the produced MoO₃ material is very fine, and after reduction, this leads to sintered Mo disks that are hard to dissolve. The advantages of the solvent extraction approach, described in Figure 3, are very high recovery yields (~98%), low waste stream volumes, and production of AHM with desired particle size.

Several large-scale extraction experiments with 140-160 g of Mo were performed using 50% TBP in 1-octanol. Solvent extraction was performed by contacting 4 L of 50% TBP in 1-octanol pre-equilibrated with 5M HCl with 4.1 L of 0.36M Mo in ~5M HCl for 2 min. After separation of the aqueous and organic phase, the organic phase was scrubbed using 2.7 L of 4.7M HCl. Finally, Mo was stripped from the organic phase using 4 L of NH₄OH (20-22% as NH₃). The strip solution was evaporated, and a solid mixture of NH₄Cl and AHM was washed (mixed by overhead stirrer) six times with ~1 L of 80% ethanol (total ~6 L).

Results are presented in Table 5. Almost 75% of the K present in the starting Mo solution in 5M KOH was removed by acidification with HCl and was collected on a glass frit. After one extraction, one scrub, and one strip, 99.97% of the K was removed, and the concentration of K in strip solution was 562 ppm. In addition, the concentration of P in the strip increased significantly, which is due to some organic-phase carryover and partial solubility of TBP in the aqueous phase. All the P introduced from the extraction was removed during the washing procedure with 80% ethanol. Moreover, this step removed a significant portion of the K, bringing the concentration of K in the final AHM product below 100 ppm. Also, 99.8% of the Na was removed. Elements like Sn and W were not removed during the recycle process, and their concentration in the target material should be, therefore, very low.

For full-scale processing of several hundred grams of Mo per day, development of an automated recycle process is very important. Annular centrifugal contactors have been used for automated solvent extraction processes for several decades mostly as part of nuclear fuel cycle research and development at U.S. Department of Energy facilities [16, 17], without any significant changes in design. However, due to the corrosiveness of hydrochloric acid, stainless steel contactors cannot be used. In this study, we tested a plastic (acrylic), 3D-printed, multi-stage centrifugal contactor (2-cm diameter) designed by Argonne [18].

Figure 6 shows the setup with 8 stages (5 extraction and three strip stages) that was originally tested. Due to some phase carryover, it was observed that a small fraction of potassium was found in the product. Therefore, in later run we used scrub stage to eliminate the presence of potassium in the organic phase before strip. The system contained five extraction stages, one scrub stage, and three strip stages. In this system, Mo was extracted from a solution of ~0.33M Mo and ~5M HCl using 30% TBP in tetrachloroethylene, scrubbed with ~4M HCl, and stripped with NH₄OH. The elemental compositions in the Mo feed, strip, and AHM product fractions, determined by inductively coupled plasma mass spectrometry (ICP-MS), are listed in Table 6. Similarly to the batch experiments (Table 5), Sn and W follow the same extraction behavior as Mo, and are not removed during the recycle process. As an alternative to Sn-stabilized peroxide, phosphate stabilized or non-stabilized peroxide should be used, since if not removed the Sn could accumulate in the recycled material.

This was the first successful demonstration of a 9-stage run with fully plastic (housing and rotor) 3D-printed centrifugal contactors, and demonstrates the feasibility of an automated extraction route for the Mo-recycle process.

Table 5. ICP-MS results for elemental composition in four fractions of solvent extraction recycle process. Results are reported with 10% uncertainty.

Element	Concentration (ppm, mg/kg-Mo)			
	Spent generator surrogate	Mo in HCl feed	Strip	AHM product
K	1.98E6	5.24E5	562	58
B	< 5.8	4.5	9.8	3.7
Na	1.08E4	1.05E4	19	19
Mg	12	27	23	21
Al	7.2	22	16	7.1
Si	< 337	199	1667	< 189
P	< 101	< 75	3.93E4	< 57
Ti	24	37	122	21
Cr	< 3.6	< 2.1	19	< 2.0
Mn	< 0.6	< 0.3	2.2	0.43
Fe	< 96	< 57	< 162	< 54
Co	< 0.1	< 0.1	< 0.2	< 0.1
Ni	< 0.5	0.46	0.94	< 0.3
Cu	5.0	5.9	7.3	12
Zn	19.3	< 5.2	100	< 5.0
Zr	< 0.3	0.89	< 0.5	0.46
Nb	1.7	2.05	1.6	1.8
Sn	7.0	22	42	50
Sb	4.2	3.2	3.91	2.2
Cs	0.8	0.58	0.67	0.34
W	206	201	132	249

Less than value (<) indicates that the concentration was below detection limit.

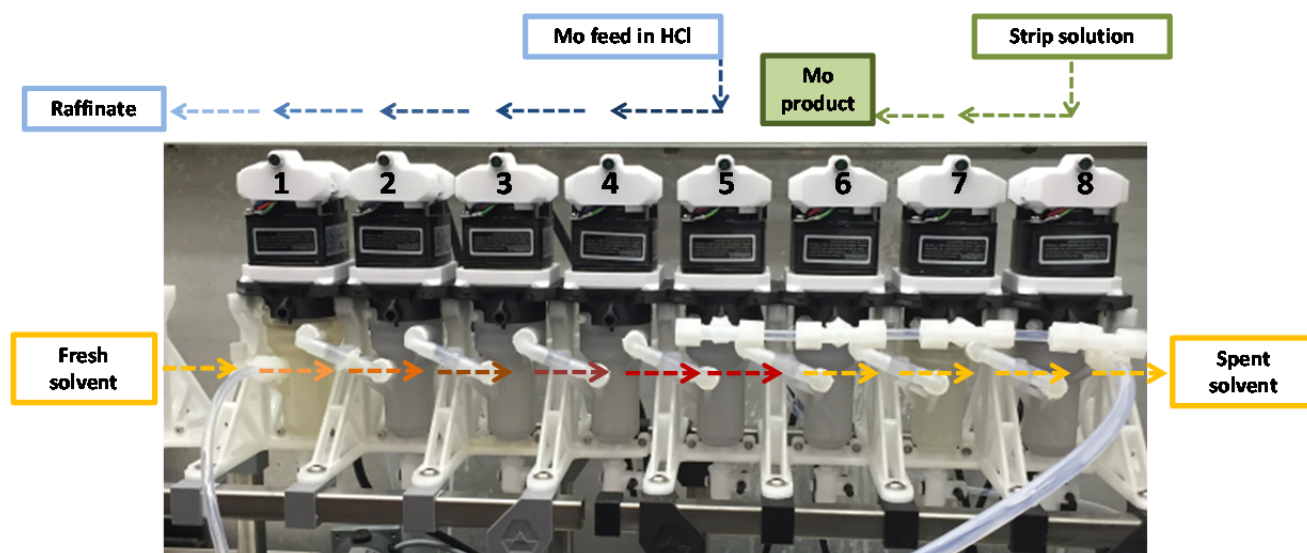


Figure 6. Eight-stage, 2-cm, 3D-printed plastic centrifugal contactors

Table 6. ICP-MS results for elemental composition in three fractions of solvent extraction recycle process using 9-stage centrifugal contactor. Results are reported with 10% uncertainty.

Element	Concentration (ppm, mg/kg-Mo)		
	Mo in HCl feed	Strip	AHM product
K	4.2E5	193	< 41
Na	2.6E3	2.7E3	< 43
P	2.5E3	2.7E3	< 111
Mg	70	133	< 19
Al	79	154	< 35
Ti	27	59	17
Fe	< 66	96	< 42
As	31	20	71
Zr	< 0.76	10	20
Nb	1.7	1.6	1.6
Cd	1.7E3	1.6E3	1.4E3
Sn	1.2E3	N/A	1.2E3
Te	97	71	79
W	3.2E3	3.0E3	2.2E3

Less than value (<) indicates that the concentration was below detection limit.

4. Acknowledgment

Work supported by the U.S. Department of Energy, NNSA's Material Management and Minimization office, and DOE-NE Fuel Cycle Technologies Program, under Contract DE-AC02-06CH11357. Argonne National Laboratory is operated for the U.S. Department of Energy by UChicago Argonne, LLC.

5. References

- [1] R.G. Bennett, J.D. Christian, D.A. Petti, W.K. Terry, S.B. Grover, "A System of ^{99m}Tc Production Based on Distributed Electron Accelerators and Thermal Separation," Nucl. Technol. 126: 102–121 (1998).
- [2] G. Dale, S. Chemerisov, G.F. Vandegrift, P. Tkac , K. Woloshun , H. Bach, C. Heath, C. Kelsey, D. Bowers, A.V. Gelis, C. Jonah, R. McCrady, E. Olivas, K. Hurtle, E. Pitcher, F. Romero, W. Tuzel, J. Giola, T. Tomei, R. Wheat, M. DeCroix, D. Warren, D. Dalmas, B. Romero, J.T. Harvey, "Global Threat Reduction Initiative (GTRI) Accelerator Production of ^{99}Mo ," Los Alamos National Laboratory Report LA-UR-11-2010.
- [3] T. Morley, K. Gagnon, P. Schaffer, E. Asselin, S. Zeisler, S. McQuarrie, M. Kovacs, J. Wilson, F. Benard, T. Ruth, "Cyclotron Production of Technetium Radioisotopes," J. Nucl. Med. 52: 291 (2011).

- [4] M.C. Lagunas-Solar, "Cyclotron Production of NCA ^{99m}Tc and ^{99}Mo , an Alternative Non-reactor Supply Source of Instant ^{99m}Tc and $^{99}\text{Mo}/^{99m}\text{Tc}$ Generators," *Int. J. Rad. Appl. Instrum. A*.42: 643–657 (1991).
- [5] S. Takacs, F. Tarkanyi, M. Sonck, A. Hermanne, "Investigation of the $\text{NatMo}(\text{p},\text{xn})^{96\text{mg}}\text{Tc}$ Nuclear Reaction to Monitor Proton Beam: New Measurements and Consequences on the Earlier Reported Data," *Nucl. Instrum. Methods Phys. Res. B*. 198: 183–196 (2002).
- [6] R. Munze, G. Hladik, G. Bernhard, W. Boessert, R. Schwarzbach, "Large Scale Production of Fission Mo-99 by Using Fuel Elements of a Research Reactor as Starting Material," *Int. J. Appl. Radiat. Isot.* 35: 749-754 (1984).
- [7] P. Tkac, D.A. Rotsch, D Stepinski, V. Makarashvili, G.F. Vandegrift, J. Harvey, "Optimization of the Processing of Mo Disks," Argonne National Laboratory Report ANL/NE-15/46 (2016).
- [8] P. Tkac, G. Vandegrift, J. Harvey, "Dissolution of Sintered Mo Disks," Argonne National Laboratory Report ANL/CSE-13/19 (July 2012).
- [9] P. Tkac, G. Vandegrift, S.D. Nunn, J. Harvey, "Processing of Sintered Mo disks Using Hydrogen Peroxide," Argonne National Laboratory Report ANL/CSE-13/44 (September 2013).
- [10] P. Tkac, G.F. Vandegrift, "Dissolution of Sintered Mo Disks," Argonne National Laboratory Report ANL/CSE-14/26 (September 2014).
- [11] M. Gumiela, J. Dudek, A. Bilewicz, "New Precipitation Method for Isolation of ^{99m}Tc from Irradiated ^{100}Mo Target," *J. Rad. Nucl. Chem.* DOI: 10.1007/s10967-016-4967-2 (2016).
- [12] D.A. Rotsch, P. Tkac, G.F. Vandegrift, "Optimization of the Dissolution of Mo Disks" Mo-99 2015 Topical meeting on molybdenum-99 Technology Development, St. Luis, Missouri (2016)
- [13] F. Benard, K.R. Buckley, T.J. Ruth, S.K. Zeisler, J. Klug, V. Hanemaayer, M. Vuckovic, X. Hou, A. Celler, J.P. Appiah, J. Valliant, M.S. Kovacs, P. Schaffer, "Implementation of Multi-curie Production of Tc-99m by Conventional Medical Cyclotrons," *J. Nucl. Med.* 55: 1017–1022 (2014).
- [14] K. Gagnon, J.S. Wilson, C.M.B. Holt, D.N. Abrams, A.J.B. McEwan, D. Mitlin, S.A. McQuarrie, "Cyclotron Production of ^{99m}Tc : Recycling of Enriched ^{100}Mo Metal Targets," *Appl. Radiat. Isot.* 70: 1685–1690 (2012).
- [15] P. Tkac, G. F. Vandegrift, "Recycle of Enriched Mo Targets for Economic Production of $^{99}\text{Mo}/^{99m}\text{Tc}$ Medical Isotope without Use of Enriched Uranium," *J. Rad. Nucl. Chem* 308: 205–212 (2016).
- [16] G. Bernstein, D. Grosvenor, J. Lenc, N.A. Levitz, "A High-Capacity Annular Centrifugal Contactor," *Nucl. Technol.* 20: 200–202 (1973).
- [17] G. Bernstein, D. Grosvenor, J. Lenc, N.A. Levitz, "Development and Performance of a High-Speed Annular Centrifugal Contactor," Argonne National Laboratory Report ANL-7969 (1973).
- [18] K.E. Wardle, "3D Printed Modular Centrifugal Contactors and Method for Separating Moieties Using 3D Printed Optimized Surfaces," United States Patent Application 20160184735.